

SUPPLEMENTARY MATERIALS OF THERMALGAUSSIAN

Anonymous authors

Paper under double-blind review

We organize the supplementary materials as follows:

- In Appendix A, we provide a detailed description of our dataset, including RGB images, thermal images, and Multi-Spectral Dynamic Imaging (MSX) images Abdullah (2023) for each scene, as well as the training and testing set divisions and relevant temperature ranges.
- In Appendix B, we provide a discussion on the limitations of this work.
- In Appendix C, we provide a discussion on its applicability.
- In Appendix D, we provide a discussion on potential future work.
- In Appendix E, we provide additional detailed results for rendering thermal images.
- In Appendix F, we include more detailed results for rendering RGB images.
- In Appendix G, We conducted comparative experiments using different modalities and multimodal images as input to estimate camera poses.
- In addition, we have included the code for this work in the folder named "ThermalGaussian_code.zip." Upon acceptance of the paper, we will make the code and dataset publicly available.

A SELF-COLLECTED THERMAL DATASET: RGBT-SCENES

As shown in table 1 and table 2, We present our dataset, which includes data from ten different scenes. This dataset contains RGB images, thermal images, and MSX images Abdullah (2023). Similarly to 3DGS Kerbl et al. (2023), we select one image from every eight for testing, with the remaining images used for training. We also provide the temperature range for the pseudo-color rendering of the thermal images.

Our dataset features scenes with varying object sizes, from large buildings and medium-sized trucks to small everyday items. It encompasses both typical daily environments and certain industrial settings. The dataset includes temperature variations ranging from a 300°C difference to a 4°C difference and covers both 360-degree and forward-facing scenarios.

This dataset utilizes the FLIR E6 Pro camera, which captures thermal images at a resolution of 240×180 pixels. The temperature measurement accuracy is $\pm 2^{\circ}\text{C}$, with an optical wavelength range of 7.5–13 μm and a temperature detection range of -20°C to 500°C . During image capture, we fixed the maximum and minimum temperatures for each scene to ensure consistent temperature readings and color representation when capturing the same location from different viewpoints.

We showcase some dynamic scenes on the anonymized website: ThermalGaussian

B LIMITATIONS

Our work builds upon the 3DGS framework to enhance multimodal and thermal field reconstruction capabilities. However, like most approaches based on 3DGS or designed for static scene reconstruction, it faces significant challenges in handling dynamic scenes, highly reflective environments, and extremely low-texture scenarios.

In many practical applications of 3D reconstruction, real-time processing is a desirable feature. While our method, like other 3DGS-based approaches, supports real-time novel view rendering, it cannot yet achieve real-time scene reconstruction. Additionally, due to the limitations of infrared

Table 1: Each scene in the RGBT-Scenes dataset is displayed


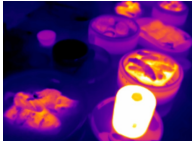
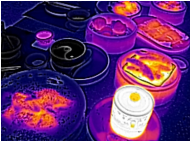

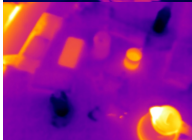
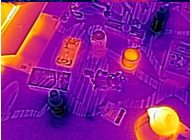

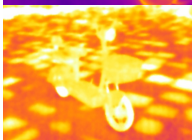


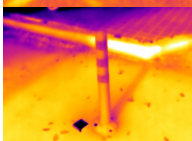
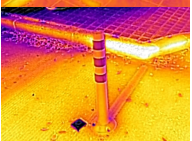





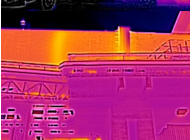

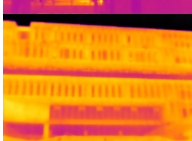
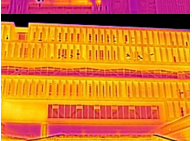

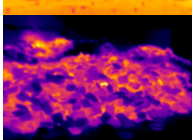
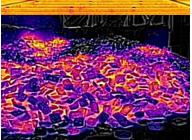

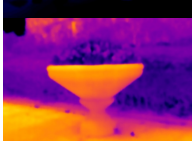
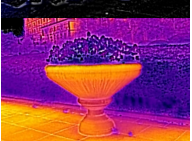

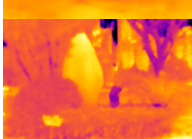





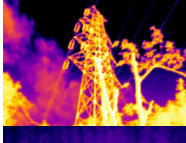
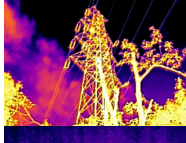

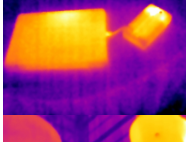
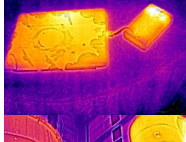

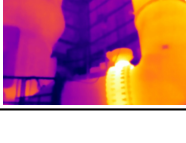

Scene	RGB	Thermal	MSX	views	Temp. range
Dimsum				134(train) 20(test)	23.1°C 60.0°C
Daily Stuff				68(train) 10(test)	17.5°C 56.3°C
Electric Bicycle				42(train) 6(test)	14.5°C 18.5°C
Roadblock				62(train) 9(test)	22.0°C 27.0°C
Truck				64(train) 9(test)	30.6°C 249.0°C
Rotary Kiln				92(train) 14 (test)	5.0°C 60.4°C
Building				238(train) 35(test)	15.0°C 24.0°C
Iron ingot				53(train) 8(test)	38.0°C 350.0°C
Parterre				57(train) 9(test)	19.5°C 27.5°C
Landscape				90(train) 13(test)	16.0°C 23.0°C

Table 2: Each scene in the expanded RGBT-Scenes dataset is displayed

Scene	RGB	Thermal	MSX	view	Temp. range
Glass Cup				123(train) 18(test)	17.0°C 36.6°C
Transmission Tower				154(train) 23(test)	-26.4°C 23.7°C
Dark Scene				75(train) 11(test)	17.5°C 21.6°C
Plant Equipment				192(train) 28(test)	27.8°C 54.9°C

thermal imaging, which can only measure the temperature of solid surfaces, our method is currently restricted to reconstructing and measuring surface temperatures rather than estimating temperatures at arbitrary points in space.

C APPLICABILITY

In **Section 2.1**, we briefly mentioned some applications of thermal imaging. We believe that any application requiring thermal imaging could benefit from establishing a 3D thermal field for better observation and analysis of temperature distributions. For example:

1. Building energy analysis: Reconstructing the 3D thermal field of a building can assist in evaluating energy efficiency.
2. Battlefield analysis: Combining 3D thermal and RGB reconstructions of localized battlefield scenarios can aid in strategic planning.
3. Equipment monitoring: Reconstructing 3D thermal fields for high-voltage power equipment or high-temperature devices can improve fault prevention and diagnosis.
4. Fire rescue: Reconstructing the 3D thermal field of fire scenes can help rescue teams devise optimal rescue strategies to save lives.

D FUTURE WORK

This work is not only a 3D reconstruction of temperature fields but also a multi-modal 3D reconstruction study. In the future, we can delve deeper into temperature field reconstruction for practical applications while also exploring 3D reconstruction in other modalities.

1. Future directions for 3D thermal field reconstruction: Currently, our method is limited to reconstructing surface temperatures. In future work, we aim to explore the reconstruction of non-surface thermal fields, including phenomena like flames. High-resolution thermal imaging devices are expensive, whereas high-resolution RGB cameras are more affordable. We plan to investigate methods for guiding low-resolution thermal image reconstruction using high-resolution RGB images, achieving results comparable to high-resolution thermal imaging while significantly reducing application costs. Many thermal processes are dynamic. To better analyze such processes, we plan to extend our work to dynamic thermal field reconstruction.

2. Future directions for multimodal reconstruction: With the advancement of technologies like the metaverse and digital twins, more objects will be digitized through 3D reconstruction. For realistic reconstruction, it is necessary to include not only geometric and color modalities but also other critical modalities, such as temperature and pressure in chemical digital twin applications. We anticipate that multimodal 3D reconstruction will become an increasingly important research direction. Moreover, multimodal reconstruction enables complementary advantages, where one modality can compensate for the limitations of another. For instance, while RGB images are less effective in low-light conditions, thermal infrared imaging remains largely unaffected. Exploring how thermal cameras can enhance nighttime 3D reconstruction is an interesting future research topic.

Meanwhile, hyperspectral imaging has extensive applications in agriculture and other fields. Future work could explore multi-modal 3D reconstruction in additional modalities.

E QUALITATIVE EVALUATION OF THERMAL IMAGES

As shown in Figure 1, we present qualitative results comparing three different multimodal Gaussian models with direct 3DGS training using thermal images based on multimodal initialization(MI). The comparison shows that incorporating the color modality into multimodal training results in significant improvements in many scenes.

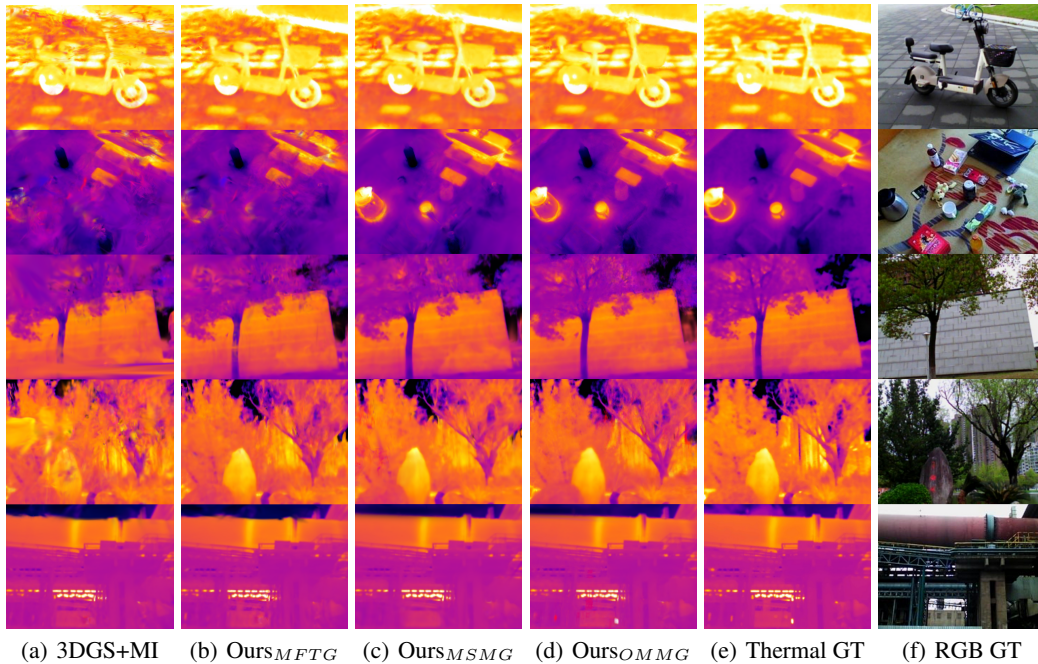


Figure 1: We present qualitative comparison results of our three multimodal Gaussian models and 3DGS+MI in rendering thermal images.

F QUALITATIVE EVALUATION OF RGB IMAGES

Our method not only enhances the rendering quality of thermal images but also improves the quality of RGB images in certain scenes, as shown in Figure 2. This improvement is particularly notable in low-light conditions and scenarios where distinguishing between foreground and background is challenging. By leveraging the thermal modality, we achieve better RGB rendering quality. Additionally, some other scenes also partial improvements.

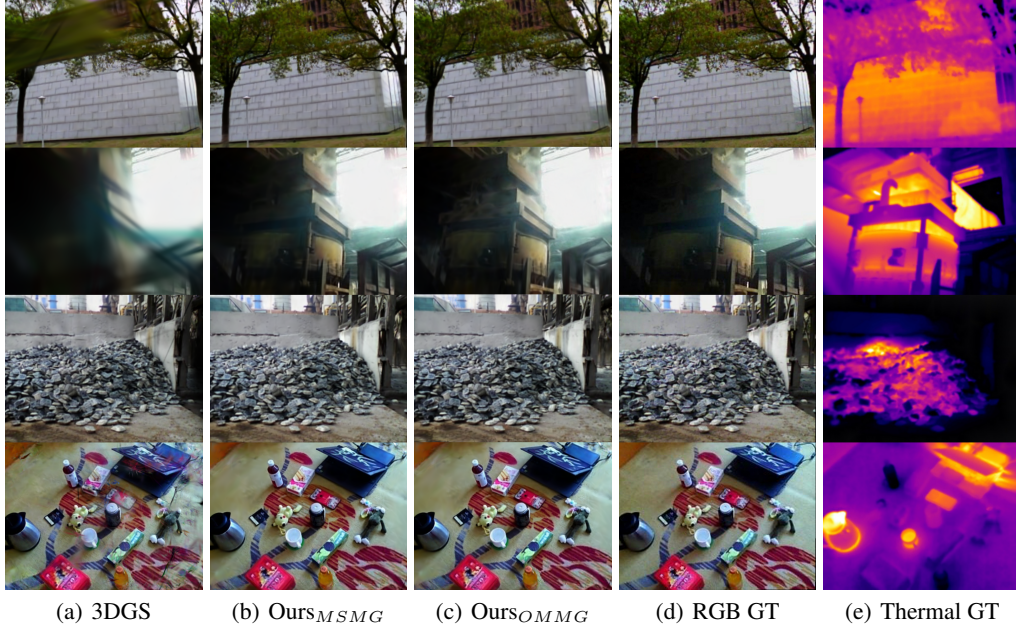


Figure 2: We present qualitative results comparing our method and 3DGS Kerbl et al. (2023) in rendering RGB images.

G QUALITATIVE EVALUATION OF RGB IMAGES

We tested different input images from Sec. 3.2 across several scenes to estimate camera poses. Subsequently, these poses were used in the baseline 3DGS for thermal field reconstruction. The quality of the estimated poses was evaluated by comparing the PSNR values of the reconstructed thermal images from novel views. As shown in table 3, the experiments demonstrate that mixing the aligned color and thermal modality images with $\beta = 0.5$ produces the most accurate camera poses.

Table 3: Comparison of different input images for camera pose estimation.

Initialization Modality	Ebike	Iron Ingot	Rotary Kiln	parterre
RGB	20.89	29.57	26.59	22.09
Mix($\beta = 0.3$)	21.09	30.15	27.11	23.02
Mix($\beta = 0.5$)	22.77	30.45	27.35	24.18
Mix($\beta = 0.7$)	\times	12.34	27.78	22.17
Thermal	\times	\times	\times	\times
MSX	22.20	29.94	27.30	24.02

REFERENCES

- Sarwin Abdullah. Low-energy radar for handheld ir-cameras: Using mmwave radar as a complement for multi spectral dynamic imaging in handheld cameras, 2023.
- Bernhard Kerbl, Georgios Kopanas, Thomas Leimkühler, and George Drettakis. 3d gaussian splatting for real-time radiance field rendering. *ACM Transactions on Graphics*, 42(4):1–14, 2023.